Journal of Power Sources 217 (2012) 43–46

Contents lists available at SciVerse ScienceDirect

Journal of Power Sources

journal homepage: www.elsevier.com/locate/jpowsour

Short communication

High power Na-ion rechargeable battery with single-crystalline $Na_{0.44}MnO_2$ nanowire electrode

Eiji Hosono [a], Tatsuya Saito [a], Junichi Hoshino [a], Masashi Okubo [a], Yoshiyasu Saito [a], Daisuke Nishio-Hamane [b], Tetsuichi Kudo [a], Haoshen Zhou [a,*]

[a] Energy Technology Research Institute, National Institute of Advanced Industrial Science and Technology, Umezono 1-1-1, Tsukuba 305-8568, Japan
[b] The Institute for Solid State Physics, The University of Tokyo, Kashiwa, Chiba 277-8581, Japan

HIGHLIGHTS

- The single crystalline $Na_{0.44}MnO_2$ nanowires for the sodium ion battery.
- The excellent cycle stability and high-charge/discharge-rate capability.
- A potential candidate for the cathode material in the high power Na-ion battery.

ARTICLE INFO

Article history:
Received 1 March 2012
Received in revised form
28 May 2012
Accepted 28 May 2012
Available online 1 June 2012

Keywords:
Nanowire
Single crystal
$Na_{0.44}MnO_2$
Sodium ion battery

ABSTRACT

High power Na-ion rechargeable batteries have attracted much interest recently. In particular, the development of nanostructured electrode materials is essentially required, because the large surface area and short Na-ion diffusion length could provide the high power density. In this paper, we report on the fabrication of single-crystalline $Na_{0.44}MnO_2$ nanowire, and the application to Na-ion rechargeable batteries. The single phase $Na_{0.44}MnO_2$ was successfully synthesized by the hydrothermal method. The SEM and TEM experiments proved that hydrothermally synthesized $Na_{0.44}MnO_2$ has single-crystalline nanowire morphology. The single-crystalline $Na_{0.44}MnO_2$ nanowire electrode in Na-ion batteries showed both the excellent cycle stability and high-charge/discharge-rate capability.

1. Introduction

Rechargeable batteries have attracted considerable attention recently because the effective use of energy and the suppression of CO_2 emissions are essential solutions to global energy and environmental problems [1]. In particular, there have been great expectations associated with the development of lithium ion batteries, i.e., large energy density [2–7]. On the other hands, sodium ion batteries are one of the post lithium ion batteries. Researchers have studied sodium ion batteries in terms of the active materials that can be used for negative and positive electrodes. The use of certain types of carbon material has been reported for the negative electrodes [8,9], while materials such as metal oxides, metal fluorides and polyanion compounds have been studied for the positive electrode [10–15].

High power rechargeable Na-ion batteries have attracted considerable interest recently, because the electric/hybrid vehicles require low cost and high power auxiliary power units. The use of abundant Na as the mobile charge could reduce the cost, while the Na-ion diffusion in the solid electrode, which is generally faster than the Li-ion diffusion, should enable the higher power output than that of the Li-ion rechargeable batteries [16]

In general, the charge-discharge process in the Na-ion battery involves three Na-ion transfer processes, *i.e.*, the Na-ion conduction in the liquid electrolyte, the Na-ion transfer at the electrolyte–electrode interface, and the Na-ion diffusion in the solid electrode. In particular, the slow ionic diffusion in the solid electrode should be the rate-limiting step when the Na-ion battery is charged/discharge at the high rate. Therefore, in order to achieve the high power Na-ion batteries, nanostructuring of the electrode materials is indispensable [17], which can reduce the Na-ion diffusion length and increase the surface area.

$Na_{0.44}MnO_2$ has been known as the cathode material for the Na-ion battery [17–19]. A tunnel structure in $Na_{0.44}MnO_2$ exhibits

* Corresponding author. Tel.: +81 29 861 5795; fax: +81 29 861 5799.
E-mail address: hs.zhou@aist.go.jp (H. Zhou).

0378-7753/$ – see front matter © 2012 Elsevier B.V. All rights reserved.
http://dx.doi.org/10.1016/j.jpowsour.2012.05.100

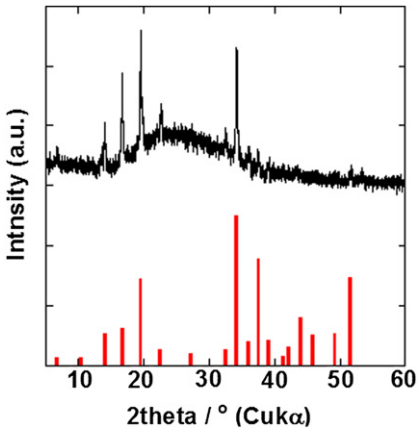

Fig. 1. XRD pattern of $Na_{0.44}MnO_2$ synthesized from the hydrothermal method.

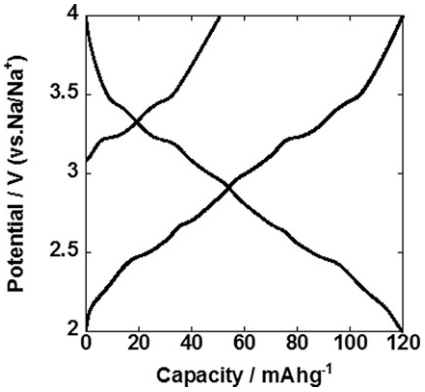

Fig. 3. Charge/discharge curves (the initial charge process and following discharge–charge cycle) for the single-crystalline $Na_{0.44}MnO_2$ nanowire at the current density of 0.05 A g^{-1} (0.42 C).

the reversible Na-ion insertion/extraction reaction. For example, rod-like $Na_{0.44}MnO_2$ synthesized from the solid state reaction was reported to show the reversible capacity of 140 mAh g^{-1} at 3.5–2.0 V vs. Na/Na^+ [19]. Cao *et al.* reported the electrode performance of the single-crystalline $Na_{0.44}MnO_2$ nanowire for the Na-ion battery, which was also synthesized from the polymer-pyrolysis method [17].

Recently, we have reported the hydrothermal synthesis of single-crystalline $Na_{0.44}MnO_2$ nanowire, and the high-charge/discharge-rate capability for the Li-ion battery [20]. In this paper, we report the application of the single-crystalline $Na_{0.44}MnO_2$ nanowire to the Na-ion battery.

2. Experimental

Single-crystalline $Na_{0.44}MnO_2$ nanowire was synthesized by the hydrothermal method. Typically, 0.1 g of Mn_3O_4 powder was dispersed in NaOH aqueous solution (40 ml, 5 mol dm^{-3}), then the solution was placed in a Teflon-lined autoclave (45 ml). The autoclave was heated at 205 °C for 96 h. After cooling the reaction solution, the precipitated powder was filtered, washed with water repeatedly, and then dried at room temperature in vacuum.

The X-ray diffraction (XRD) measurement was carried out with a Bruker AXS D8 Advance using Cu Kα radiation. The morphology was observed by the field emission scanning electron microscopy (FE-SEM) and bright field transmission electron microscopy (bright field TEM) using a Carl Zeiss Supra 35 microscope and a JEOL JEM-2010F (200 kV accelerating voltage), respectively. The specific surface area was estimated by the BET method based on the N_2 adsorption using Micromeritics Tristar 3000.

Electrochemical properties were evaluated with a three-electrode glass cell. The $Na_{0.44}MnO_2$ nanowire was ground with 5 wt% Teflon and 45 wt% acetylene black. The capacity of acetylene black is too small. So, the capacity in this paper is almost based on $Na_{0.44}MnO_2$. The mixture was then spread and pressed onto an SUS-304 mesh (100 mesh) as a working electrode. The reference and counter electrodes were prepared by spreading and pressing sodium metals onto an SUS-304 mesh (100 mesh). 1 mol dm^{-3} of $NaClO_4$ in PC was used as the electrolyte. Cell assembly was carried out in a glove box under an argon atmosphere. The specific capacity (mAh g^{-1}) and specific current (A g^{-1}) were calculated with the weight of the active material.

3. Results and discussion

Single-crystalline $Na_{0.44}MnO_2$ nanowire was synthesized by the hydrothermal method as previously described in the literature [20,21].

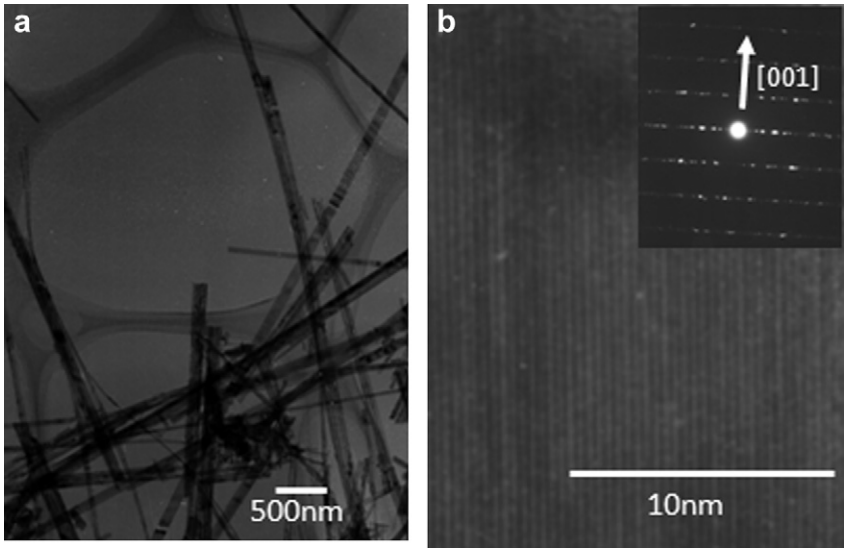

Fig. 2. (a) Bright field TEM image and (b) the high resolution bright field TEM image of hydrothermally synthesized $Na_{0.44}MnO_2$. The inset in (b) shows the selected area electron diffraction pattern.

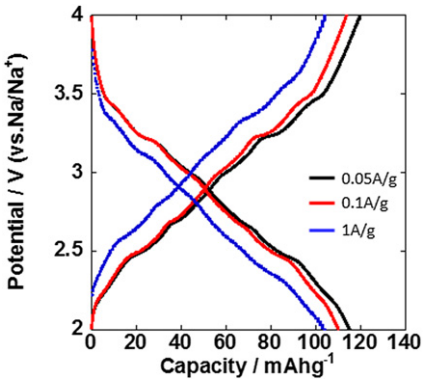

Fig. 4. Charge/discharge curves in 2nd cycle of the single-crystalline $Na_{0.44}MnO_2$ nanowire at 0.05 A g^{-1} (0.42 C), 0.1 A g^{-1} (0.83 C), and 1 A g^{-1} (8.3 C).

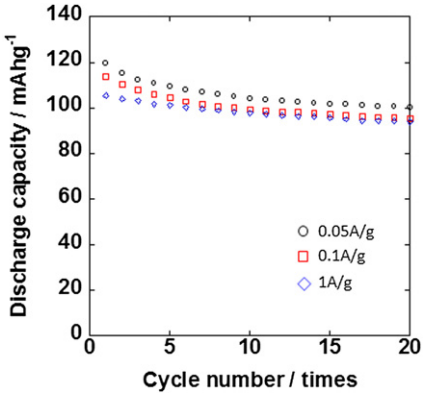

Fig. 5. Cycle performance of the single-crystalline $Na_{0.44}MnO_2$ nanowire at 0.05 A g^{-1} (0.42 C), 0.1 A g^{-1} (0.83 C), and 1 A g^{-1} (8.3 C).

Fig. 1 shows the XRD pattern of the resulting material. The XRD pattern well agrees with that of $Na_{0.44}MnO_2$ (JCPDS No. 27–0570), which suggests the successful formation of a $Na_{0.44}MnO_2$. The peaks can be indexed into orthorhombic *Pbam*, and the calculated unit cell parameters ($a = 9.081$, $b = 26.15$, $c = 2.822$) are almost consistent to the previously reported values ($a = 9.078$, $b = 26.44$, $c = 2.827$) [19]

Fig. 2(a) shows the bright field TEM image for the hydrothermally synthesized $Na_{0.44}MnO_2$. The nanowire morphology with the high aspect ratio ($>\sim 50$) is clearly imaged. Both a clear lattice image in the high resolution bright field TEM image in Fig. 2(b) and sharp diffraction spots in the selected area electron diffraction pattern in the inset of Fig. 2(b) suggest the single-crystalline nature in one-dimensional direction. The surface area was estimated to be 28.2 m^2 g^{-1} by the BET method on the basis of N_2 adsorption and desorption isotherms at 77 K. This value is much higher than 17.8 m^2 g^{-1} for $Na_{0.44}MnO_2$ synthesized from the polymer-pyrolysis method [17], which clearly demonstrates the advantage of the non-woven fabric structure with the nanowires. All these results confirmed that the hydrothermal product is the single-crystalline $Na_{0.44}MnO_2$ nanowire.

The single-crystalline $Na_{0.44}MnO_2$ nanowire was applied to the cathode material in the Na-ion battery. Fig. 3 shows the charge/discharge curves (the initial charge process and following discharge–charge cycle) for the single-crystalline $Na_{0.44}MnO_2$ nanowire at the current density of 0.05 A g^{-1}. The initial charge capacity was 50 mAh g^{-1} corresponding to 0.18 Na-ion extraction from $Na_{0.44}MnO_2$, in which the potential plateaus were observed at 3.2 and 3.45 V. These potential plateaus could be ascribed to the Na-ion extraction via the two phase process, which has been reported to exist at the composition range of $0.28 < x < 0.32$ and $0.38 < x < 0.42$ [19]. The following discharge–charge cycle provides the reversible charge/discharge capacity of 120 mAh g^{-1}, which implies 0.43 Na-ion insertion/extraction in Na_xMnO_2 ($0.26 < x < 0.69$). In addition to above mentioned two potential plateaus at 3.45 and 3.2 V, four potential plateaus at 3.0, 2.6, 2.5 and 2.2 V were observed during both charge and discharge processes. These potential plateaus could also be explained by the Na-ion insertion/extraction via the two-phase process, because the Na-ion insertion into $N_{0.44}MnO_2$ exhibits the two-phase state at the composition range of $0.28 < x < 0.32$, $0.38 < x < 0.42$, $0.48 < x < 0.50$, and $0.54 < x < 0.57$ [19].

Generally speaking, Na-ions in Na_xMnO_2 could occupy two sites, *i.e.*, the A-site in the large S-shaped tunnel and the B-site in the small tunnel. Sauvage *et al.* reported that Na-ions could be reversibly inserted/extracted into/from the A-site, while Na-ions at

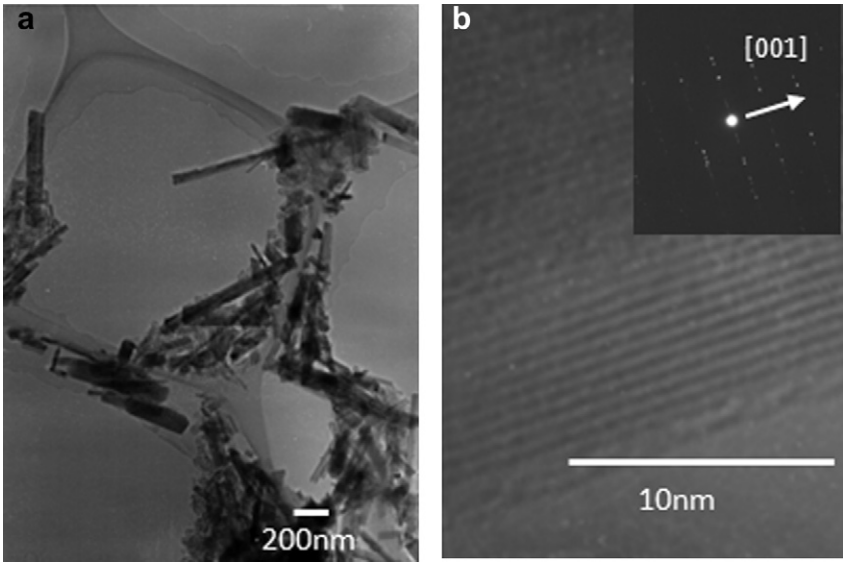

Fig. 6. (a) Bright field TEM image and (b) high magnification bright field TEM images of $Na_{0.44}MnO_2$ nanowires after 20 cycles at 1 A g^{-1} (8.3 C). The inset in (b) is the selected area electron diffraction pattern.

the B-site could hardly be extracted in the potential range of 2–3.8 V [19]. The coexistence of the active and inactive sites in the host results in the electrochemical reaction as,

$$0.44Na^{+} + 0.44e^{-} + Na_{0.22}MnO_2 \leftrightarrows Na_{0.66}MnO_2,$$

in which all of the Na-ions could not be extracted. The observed electrochemical reaction for the single-crystalline $Na_{0.44}MnO_2$ nanowire well agrees with the above reaction.

Fig. 4 shows the charge/discharge curves during the 2nd charge-discharge cycle at various charge-discharge rates. The reversible capacity was 115 mAh g^{-1}, 110 mAh g^{-1}, and 103 mAh g^{-1} at the specific current of 0.05 A g^{-1} (0.42 C), 0.1 A g^{-1} (0.83 C), and 1 A g^{-1} (8.3 C), respectively. The capacity loss was only 10% even at 8.3 C, which clearly proves the high-charge/discharge-rate capability of the single-crystalline $Na_{0.44}MnO_2$ nanowire for the Na-ion batteries.

The single-crystalline $Na_{0.44}MnO_2$ nanowire showed high cycle stability as shown in Fig. 5. The charge/discharge capacity loss was only 12% at 8.3 C rate after 20 cycles. In order to clarify the origin of the high cycle stability, the bright field TEM was imaged after 20 cycles at 8.3 C rate (Fig. 6). The lattices based on the wall plane of the nanowires were clearly imaged, and the selected area electron diffraction pattern indicated the single-crystalline nature in the one-dimensional direction. Thus, the robust host structure of $Na_{0.44}MnO_2$, which could be maintained after the Na-ion insertion/extraction, should be one of the origins for the high cycle stability of the single-crystalline $Na_{0.44}MnO_2$ nanowire.

4. Conclusions

We have reported the fabrication of the single-crystalline $Na_{0.44}MnO_2$ nanowire, and its application to the cathode material of the Na-ion battery. The single-crystalline $Na_{0.44}MnO_2$ nanowire, which was synthesized from the hydrothermal method, showed the reversible capacity of 120 mAh g^{-1}. The observed charge/discharge process including six two-phase states well agreed with that for the previously reported $Na_{0.44}MnO_2$ synthesized from the solid state reaction. Furthermore, the single-crystalline $Na_{0.44}MnO_2$ nanowire showed the high-charge/discharge-rate capability and high cycle stability, which suggested that the single-crystalline $Na_{0.44}MnO_2$ nanowire is a potential candidate for the practical cathode material in the high power Na-ion battery.

Acknowledgment

This work was partially performed using facilities of the Institute for Solid State Physics, the University of Tokyo.

References

[1] M. Armand, J.-M. Tarascon, Nature 451 (2008) 652.
[2] B. Ammundsen, J. Paulsen, Adv. Mater. 13 (2001) 943.
[3] Z. Li, F. Du, X.F. Bie, D. Zhang, Y.M. Cai, X.R. Cui, C.Z. Wang, G. Chen, Y.J. Wei, J. Phys. Chem. C 114 (2010) 22751.
[4] Z.H. Lu, L.Y. Beaulieu, R.A. Donaberger, C.L. Thomas, J.R. L Dahn, J. Electrochem. Soc. 149 (2002) A778.
[5] A.D. Robertson, P.G. Bruce, Chem. Mater. 15 (2003) 1984.
[6] M.M. Thackeray, S.H. Kang, C.S. Johnson, J.T. Vaughey, R. Benedek, S.A. Hackney, J. Mater. Chem. 17 (2007) 3112.
[7] N. Yabuuchi, K. Yoshii, S.-T. Myung, I. Nakai, S. Komaba, J. Am. Chem. Soc. 133 (2011) 4404.
[8] S. Komaba, T. Itabashi, M. Watanabe, H. Groult, N. Kumagai, J. Electrocchem. Soc. 154 (2007) A322.
[9] R. Alcántara, J.M. Jiménez-Mateos, P. Lavela, J.L. Tirado, Electrochem. Commun. 3 (2001) 639.
[10] Y. Uebou, S. Okada, J. Yamaki, J. Power Sources 115 (2003) 119.
[11] S. Komaba, T. Mikumo, A. Ogata, Electrochem. Commun. 10 (2008) 1276.
[12] I.D. Gocheva, M. Nishijima, T. Doi, S. Okada, J. Yamaki, T. Nishida, J. Power Sources 187 (2009) 247.
[13] H.T. Zhuo, X.Y. Wang, A.P. Tang, Z.M. Liu, S. Gamboa, P.J. Sebastian, J. Power Sources 160 (2006) 698.
[14] T. Shiratsuchi, S. Okada, J. Yamaki, T. Nishida, J. Power Sources 159 (2006) 268.
[15] Z. Jian, L. Zhao, H. Pan, Y.S. Hu, H. Li, W. Chen, L. Chen, Electrochem. Comm. 14 (2012) 86.
[16] P.G. Bruce, Solid State Electrochemistry, Cambridge University Press, 1995.
[17] Y. Cao, L. Xiao, W. Wang, Da. Choi, Z. Nie, J. Yu, L.V. Saraf, Z. Yang, J. Liu, Adv. Mater. 23 (2011) 3155.
[18] M.M. Doeff, S.J. Visco, Y.P. Ma, M. Peng, L. Ding, L.C. De Jonghe, Electrochim. Acta 40 (1995) 2205.
[19] F. Sauvage, L. laffont, J.M. Tarascon, E. Baudrin, Inorganic. Chem. 46 (2007) 3289.
[20] E. Hosono, H. Matsuda, I. Honma, S. Fujihara, M. Ichihara, H.S. Zhou, J. Power Sources 182 (2008) 349.
[21] E. Hosono, T. Kudo, I. Honma, H. Matsuda, H.S. Zhou, Nano Lett. 9 (2009) 1045.